

Properties Investigation of Fullerene/GNPs Composite Films

Lara S. Khalil* and Mazin A. Alalousi

Department of Physics, College of Science, University of Anbar, Ramadi, IRAQ



ARTICLE INFO

Received: 31 / 01 /2024
Accepted: 23 / 04 / 2024
Available online: 31 /12 /2024

[10.37652/juaps.2024.146514.1188](https://doi.org/10.37652/juaps.2024.146514.1188)

Keywords:

Fullerene, Laser ablation, Electro spray, PL, UV-VIS.

Copyright©Authors, 2022. College of Sciences, University of Anbar. This is an open-access article under the CC BY 4.0 license (<http://creativecommons.org/licenses/by/4.0/>).



ABSTRACT

Fullerene–gold nanoparticle (GNP) composite films were prepared via laser ablation and electrospray techniques. A pulsed Nd-YAG laser with a wavelength of 1064 nm and an energy of 100 mJ was used to prepare colloidal solutions, which were sprayed onto quartz substrates using an electrospray device at temperatures of 300 ± 20 °C. The prepared films were characterized through X-ray diffraction, scanning electron microscopy, ultraviolet-visible spectrophotometry, and photoluminescence (PL) to investigate their structural, morphological, and optical properties, respectively. The prepared films showed multiple phases of C60 and C70, with differences in distribution observed based on the concentration of GNPs. In addition, several gap energies, whose values ranged from 1.95 eV to 5.62 eV based on the formation phase, were detected for each film based on their absorption behavior within the wavelength range of 200–900 nm. In addition, the PL spectra exhibited four peaks for each film, with the concentration of GNPs affecting the positions of emission peaks and the appearance of peaks beyond 500 nm coinciding with the addition of gold to the compound.

Introduction

The chemical element carbon has an atomic number equal to 6, is located at the top of group IV, the carbon group, and belongs to the second-period elements in the periodic table. Carbon is a simple and stable element and found in high abundance. This element ranks fourth in terms of the highest abundance in the universe. Carbon has a high capability to engage in covalent bonding[1,2, 3]. It was previously known to exist in two main allotropes, namely, diamond and graphite. Later, several other forms carbon were discovered. The various forms of carbon can be attributed to its three hybridizations (sp , sp^2 , and sp^3), such as those observed in diamond, graphene, carbon nanotubes, and carbon fibers. However, each formation has its own characteristics because of the unique bonding of atoms[4]. Given the abundance of carbon and its unique properties, it has attracted great research attention and has been included in industries, such as sensors, solar cells, and others[2]. Distinctively, this material can absorb electrons and metal atoms inside surfaces and balance them with respect to ultraviolet-visible (UV-VIS) wavelengths (the breadth of its absorption of light in this region)[5]

it also possesses unique mechanical and electronic properties, including a strong van der Waals interaction and a large surface-to-volume ratio, that enable its application in the manufacture of numerous nanodevices [6]. Fullerene was first introduced in 1985[7]; this form of carbon is sp^2 hybridized, has a nanostructure, and has received great attention due to the importance of its structure and its involvement in various scientific fields[8]. The most important feature of fullerene is its high conductivity (33 K). This carbon form is also distinguished by its pentagonal symmetry and icosahedral shape[9]. The spherical, cage-like shape of fullerene has aroused great interest among researchers. In addition, fullerene is very small in size and takes different shapes, such as completely or partially closed carbon networks, which consist of carbon atoms linked together by single or double bonds and form rings usually comprising 5 to 7 atoms[10]. The initial assumption for fullerenes, especially C60, originated from some Russian scientists, who proposed that C60 possesses a large electronic gap between the highest occupied molecular orbital and the lowest unoccupied

*Corresponding author at : Department of Physics, College of Science, University of Anbar, Ramadi, IRAQ
ORCID:<https://orcid.org/0000-0000-0000-0000>,
Tel: +964 7000000000
Email: lar21s2004@uoanbar.edu.iq

molecular orbital. This notion stemmed from Osawa's suggestion that this molecule is chemically stable[2]. Given its distinct chemical and physical properties, such as its association with carbon compounds, noble metals, and other materials, in addition to its controllable optical gaps, fullerene has been used in many applications[11]. Despite the importance of this carbon type and its inclusion in various applications and industries, numerous challenges, especially those associated with its manufacture and production, the very small quantities of fullerene produced compared with the need for its use in a number of applications, and its high cost, remain[12,13]. Four main methods are used to synthesize fullerene: electric arc heating of graphene, laser irradiation of carbon, resistive arc heating of graphene, and laser irradiation of polyromantic hydrocarbons[14]. Pulsed laser ablation in liquid (PLAL) is one of the most important and popular techniques for the preparation of nanoparticle (NP) colloidal; fullerene colloidal in various organic and inorganic liquids have been prepared via the PLAL technique[15-19]. Fullerenes have distinctive and unique optical properties that can be identified through their photoluminescence (PL) and UV-VIS spectra. These materials are characterized by multiple absorption regions (404, 535, 570, 591, and 625 nm) resulting from $\pi \rightarrow \pi^*$ and $n \rightarrow \pi^*$ transitions. Several vibrational excitations are activated through the HT coupling orbital to the distorted JT orbital at a higher level, which provides a broadband for fullerenes[4]. Therefore, this study aimed to study the optical properties of previously prepared fullerene/gold NP (GNP) composite films[19].

Materials and Method

Fullerene/GNP composite films were prepared as reported in our previous study[19]. Batteries with carbon electrodes were utilized as raw precursors to prepare fullerene colloidal and gold pellet to prepare (GNPs) colloidal in distilled water using a pulsed Nd-YAG laser

with a wavelength of 1064 nm. Fullerene and GNP colloidal (0.412, 1.944, and 3.575 ppm) were mixed and electrospayed onto quartz substrates at substrate temperatures of 250 ± 25 °C. The structural properties of the prepared films were determined and analyzed. Meanwhile, their morphological properties and thickness were obtained using field-emission scanning electron microscopy (FESEM) images. Optical properties were achieved by studying the UV-vis (200–900 nm) and PL spectra (250–550 nm). The band gaps of the prepared films were evaluated utilizing the Tauc plot.

Results and discussion

X-Ray diffraction (XRD) patterns (Fig. 1) revealed the multiphase crystalline structures of the prepared films and the concentration effect of the added gold particles. The C_{60} (311) phase dominated at 20.77° in the films prepared without gold. Mixing with gold particles at a concentration of 0.412 ppm led to the dominance of C_{70} (600) at 20.17° . On the other hand, when the amount of gold was increased to 1.944 ppm, the dominant phase was C_{70} at 21.45° . Likewise, at the 3.573 ppm concentration of gold, the C_{70} phase (132) showed a dominance with a slight shift in location (1.52°).

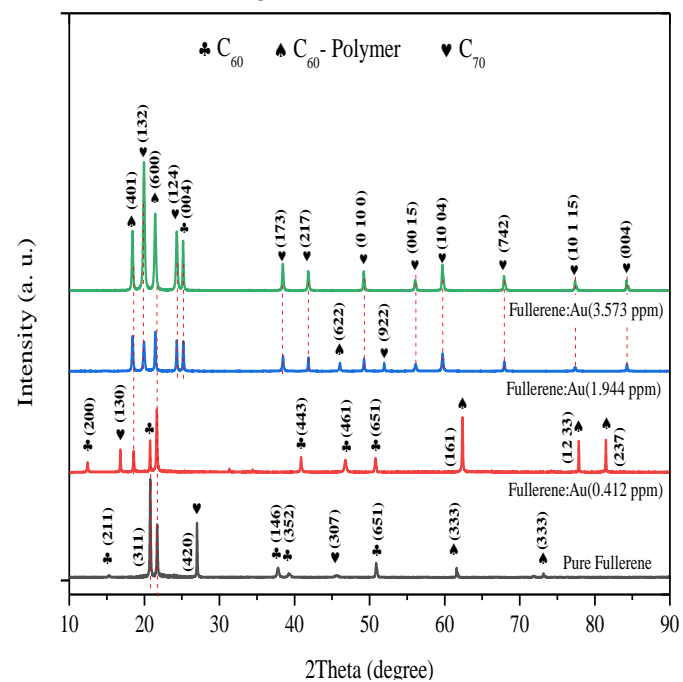


Figure. 1: XRD patterns of the prepared fullerene/GNP films

The FESEM images (Fig. 2) confirmed that the surface of the fullerene films contained rod clusters with an average diameter of approximately 300 nm. Moreover, the addition of GNPs at concentrations of 0.412, 1.944, and 3.575 ppm affected the formation and distribution of surface particles, consistent with the XRD patterns. Various shapes and sizes, such as spherical particles, rods, and rocks (assumed to be a part of graphite that remained and were larger than 300 nm), distinguished each film depending on the concentration of GNPs. This variation in shape and distribution was due to several reasons, such as the formation of C₆₀ polymer, local differences in the temperature and electric field intensity, segregation of impurity and variations in surface energy values. Meanwhile, the thickness of film swings with sizes of 1.87, 3.6, 0.563, and 0.679 μm were observed for the fullerene/GNPs at 0.412, 1.944, and 3.575 ppm, respectively (reduced images in Figure 2).

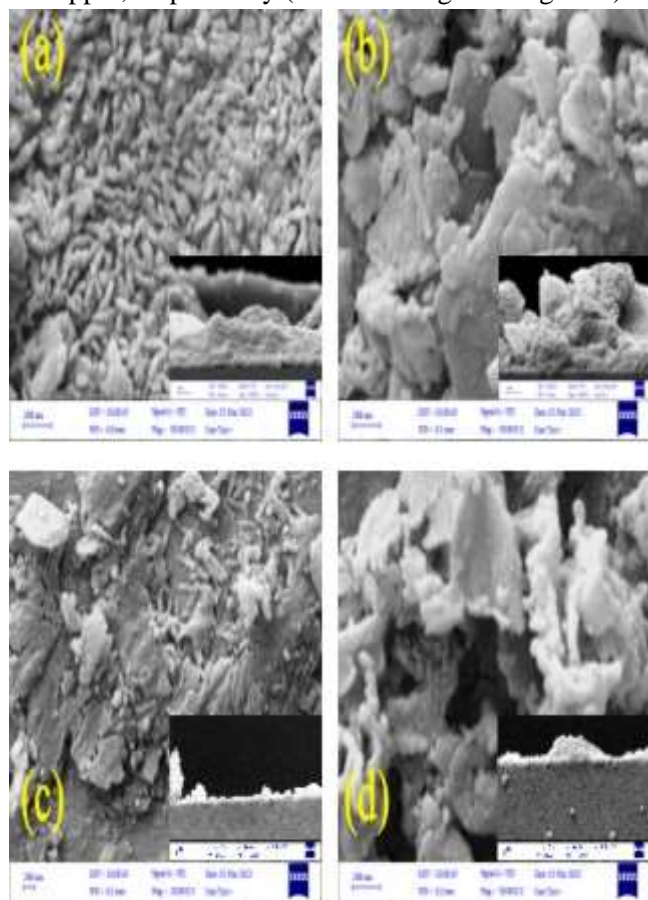


Figure. 2 : FESEM of the prepared fullerene/GNP films. (a) Fullerene, (b) fullerene:Au (0.412 ppm), (c) fullerene:Au (1.944 ppm), and (d) fullerene:Au (3.575 ppm)

Figure 3 illustrates the absorbance spectra of the prepared films. The pure-carbon film showed peaks at wavelengths of 210, 225, 275, and 379 nm, which fall within the UV region. These peaks proved the presence of fullerene, which has 30 double bonds and causes π - π^* transition due to C=C. This outcome indicates the presence of nanocarbon particles within these limits[17,20,21]. In this study, the peaks slightly blue shifted compared with previous studies, and this finding was attributed to hydrogen bond formation due to the presence of water[22]. In general, the amount of GNPs was increased. The addition of GNPs resulted in a nonuniform increase in absorbance intensities. The absorption spectrum of the fullerene films showed the appearance of peaks at 219, 274, and 350 nm. Changes in the sites of recognized peaks was caused by the presence of impurities given that the raw material had a low purity (dry batteries residues), as previously referred to in the discussion of XRD patterns. Gold was not detected directly in the XRD patterns due to the small concentrations of GNPs in the prepared compound. However, the inclusion of gold in the composition of the prepared overlay resulted in the emergence of a distinctive peak of the surface plasmon resonance of GNPs, which appeared at around 520 nm. This peak changed depending on the particle size and the surrounding medium. The values changed to 544, 546, and 548 nm at concentrations of 0.412, 1.944, and 3.575 ppm, respectively. This finding indicates an increase in the size of gold particles due to aggregation and an alteration in the concentration of the surrounding carbon particles. In addition, the peaks of fullerenes, shift in their positions, and intensity were observed as the concentration of gold particles changed. The presence of gold in the XRD patterns is inevident in the absorption spectrum due to the small concentrations of GNPs in the prepared composite.

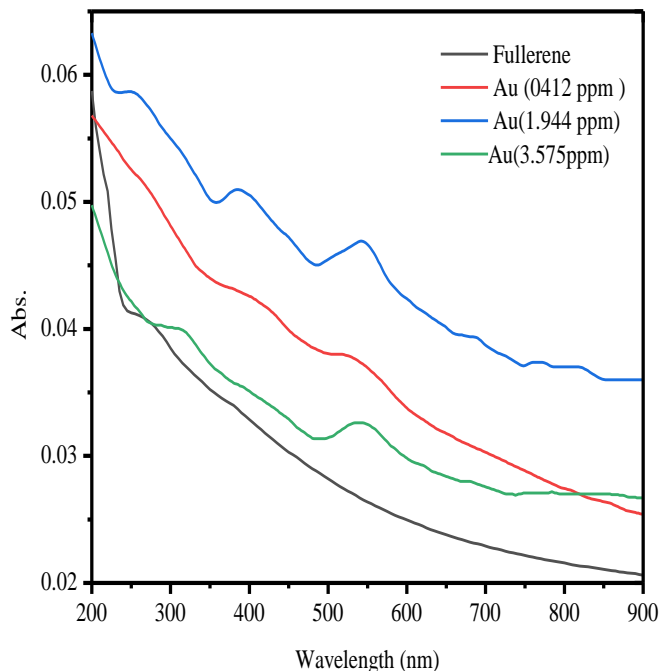


Figure 3. Absorbance of the prepared fullerene/GNP films

Given the small intensity of the peaks in the fullerene absorption spectrum, we redrew the spectrum individually and focused on the weak peak at 379 nm in Figure 4.a. The fullerene film had three energy gaps at 4.25, 2.6, and 1.95 eV, as presented in Figures 4(a and b).

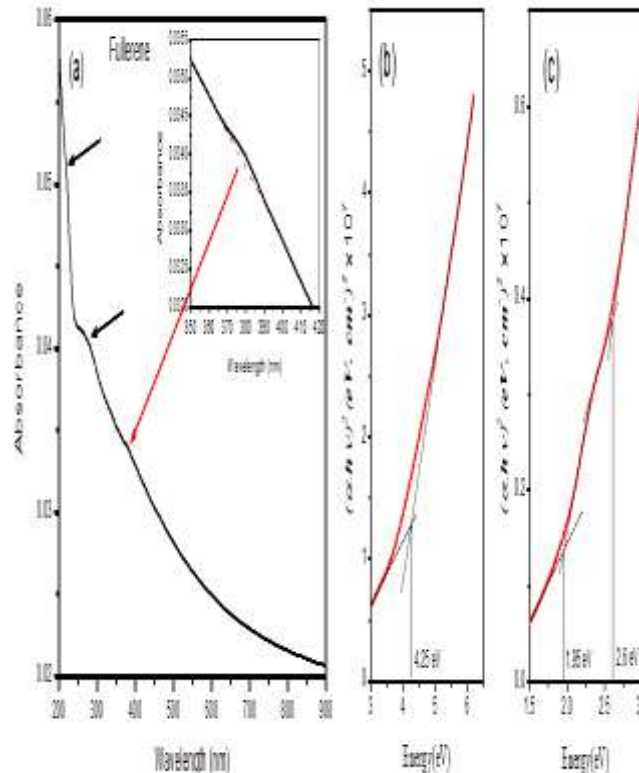


Figure 4 (a) Absorbance of the prepared fullerene film (b) and (c) plots of $(\alpha h\nu)^2$ of the fullerene film against photon energy

As shown in Figure 5, the increase in the concentration of GNPs led to changes in the energy gap values, with the 1.95 eV gap initially disappearing at the concentration of 0.412 ppm and then reappearing at the higher two concentrations with a slight modification. Moreover, the energy gap of 4.25 eV shifted to 594, 562, and 5.60 eV, which was achieved based on the increased concentration of GNPs; this outcome resulted from the contribution of GNPs in the generation of subenergy states and increased elongation in fullerene particles[23-25].

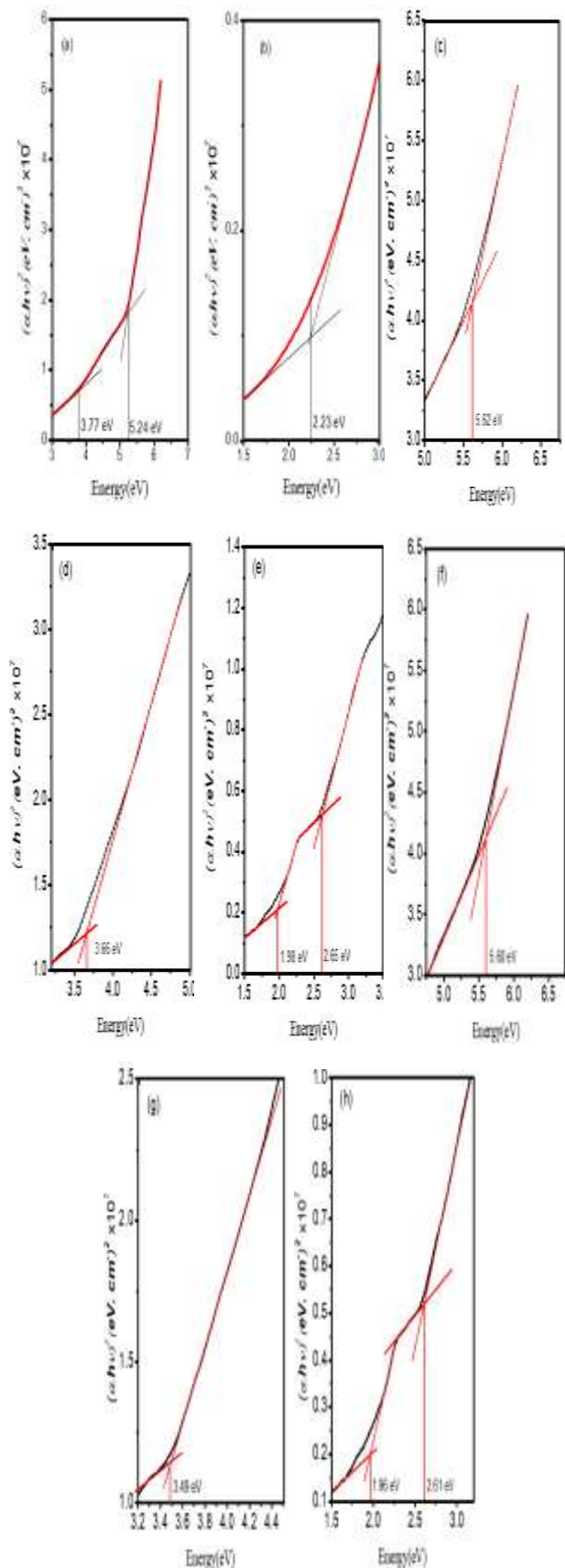


Figure. 5 Fig. 5 Plots of $(\alpha h\nu)^2$ of fullerene/GNP film against photon energy

The absorption of specific light energy can cause an imbalance in the electron population. PL is produced due to the downshift of electrons from higher states to lower states [26]. In addition, PL represents an effective indicator for quality, transitions, and identification of defects in semiconductors [27]. The PL behavior of fullerenes is subject to several considerations, such as multiple symmetry and Jahn–Teller distortions[28]. In this work, fullerene:GNP films were excited by laser wavelengths of 280 and 320 nm. As shown in Figures 6(a and b), the fullerene film showed peaks at 337, 347.7, 411, 438.3, and 484.9 nm, with excitation by a wavelength of 280 nm. Meanwhile, those excited at a wavelength of 320 nm showed an emission represented by a peak at 562 nm, which may be related with $H_u \rightarrow T_{1g}$ [4].

The first peak (337 nm) redshifted with the increase in the GNP concentration addition to the increase in its intensity within 0.412 and 1.944 ppm of GNP concentrations. However, it receded at the concentration of 3.575 ppm. The increased concentration of GNPs affected the behavior of the PL spectrum of the composite. This condition led to a red shift at both concentrations and a decline at the concentration of 3.575 ppm. This finding was due to changes in the shapes, sizes, and phases of the formed structures, as explained in the discussion on XRD and SEM images on a previous site[29]. The emission peaks of GNPs depend on the excitation energy, but they fall within the 400–650 nm region and is related to the highly enhanced two-photon luminescence for gold nanorods[30]. Therefore, the emissions at 520.2, 539.2, and 507.8 nm can be attributed to gold nanorods. Subsequently, the films excited at the wavelength of 320 nm maintained the position of the emission peak but suffered a suppression in the intensity, which can be attributed to the increased accumulation of fullerene. Figure 6 and Table 1 illustrate the emission peaks of the prepared fullerene/GNP films.

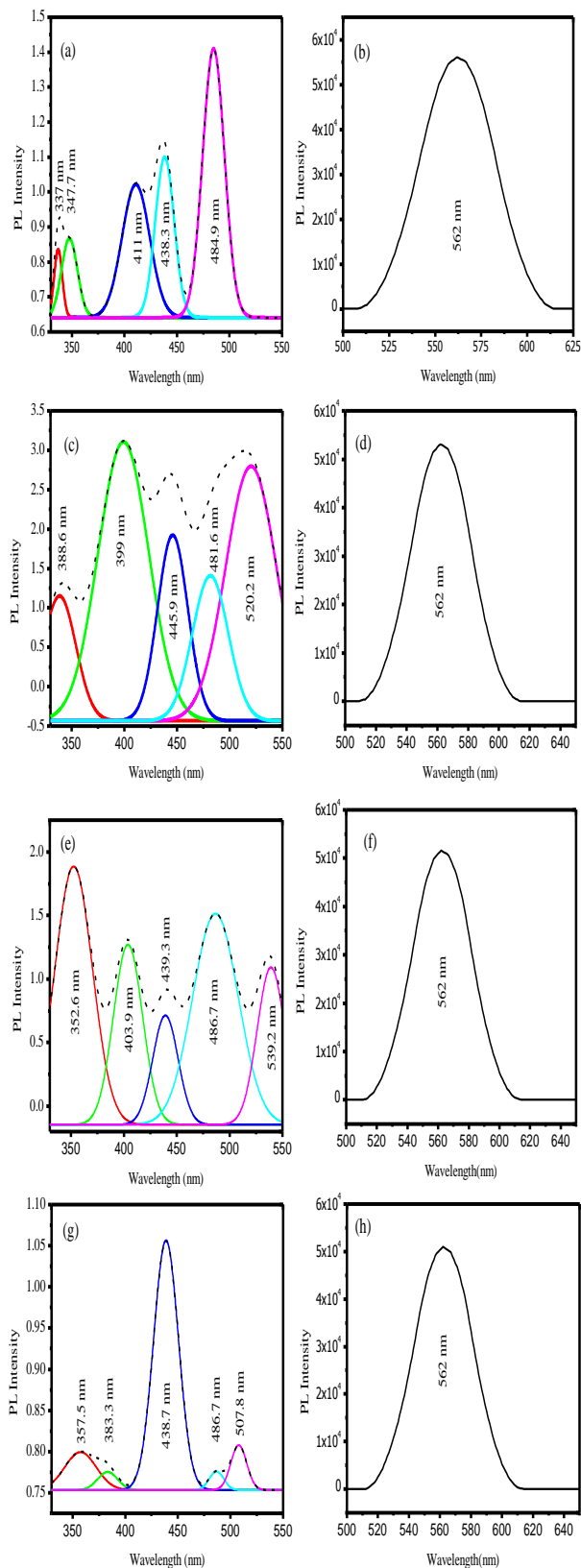


Figure 6 Emission peaks of the prepared fullerene/GNP films

Table 1. Emission peaks of the prepared fullerene/GNP films

Peak No.	Fullerene	GNPs 0.412 ppm	GNPs 1.944 ppm	GNPs 3.575 ppm
Peak1	337	338.6	352.6	357.5
Peak2	347.7	399.2	403.9	383.3
Peak3	410.9	445.9	439.3	438.7
Peak4	438.3	481.6	486.7	486.7
Peak5	484.8	520.2	539.2	507.8

Conclusion

The use of laser ablation and electro spraying are considered an effective approach to the preparation of C₆₀ and C₇₀ fullerenes. In addition, the inclusion of GNPs within certain limits enhanced the optical properties of these fullerenes by contributing to the plasmon resonance of the GNPs, depending on the optical excitation wavelength. When excited at a wavelength of 280 nm, the PL activity and redshift were enhanced at weak concentrations in the region of 300–550 nm. However, an increase in concentration led to the suppression of intensity while maintaining the location of the emission peak excited at a wavelength of 320 nm in the region beyond 500 nm.

References

- [1] Meunier, V., Ania, C., Bianco, A., Chen, Y., Choi, G.B., Kim, Y.A., et al. (2022) "Carbon Science Perspective in 2022: Current Research and Future Challenges." *Carbon*. 195 272–291.
- [2] Wu, M., Liao, J., Yu, L., Lv, R., Li, P., Sun, W., et al. (2020) "2020 Roadmap on Carbon Materials for Energy Storage and Conversion." *Chemistry - An Asian Journal*. 15 (7), 995–1013.
- [3] Georgakilas, V., Perman, J.A., Tucek, J., and Zboril, R. (2015) "Broad Family of Carbon Nanoallotropes: Classification, Chemistry, and Applications of Fullerenes, Carbon Dots, Nanotubes, Graphene, Nanodiamonds, and Combined Superstructures." *Chemical Reviews*. 115 (11), 4744–4822.
- [4] Saraswati, T.E., Setiawan, U.H., Ihsan, M.R., Isnaeni, I., and Herbani, Y. (2019) "The Study of the Optical Properties of C₆₀ Fullerene in Different Organic Solvents." *Open Chemistry*. 17 (1), 1198–1212.

- [5] Watson, H., Cockbain, A.J., Spencer, J., Race, A., Volpato, M., Loadman, P., et al. (2016) "Author's Accepted Manuscript Author's Accepted Manuscript." Prostaglandins, Leukotrienes and Essential Fatty Acids. 115 60–66.
- [6] Gao, Z. and Zhao, K. (2010) "Minimal Realization of Linear System Based on New Smith-McMillan Normal Form of Transfer Function Matrix." Advances in Systems Science and Applications. 10 (3), 531–537.
- [7] Thakral, S. and Mehta, R. (2006) "Fullerenes: An Introduction and Overview of Their Biological Properties." Indian Journal of Pharmaceutical Sciences. 68 (1), 13–19.
- [8] Saito, R., Hofmann, M., Dresselhaus, G., Jorio, A., and Dresselhaus, M.S. (2011) "Raman Spectroscopy of Graphene and Carbon Nanotubes." Advances in Physics. 60 (3), 413–550.
- [9] Dresselhaus, M.S., Dresselhaus, G., and Eklund, P.C. (1993) "COMMENTARIES AND REVIEWS Fullerenes."
- [10] Ota, N. (1904) "Graphene Molecule Compared With Fullerene C60 As Circumstellar Carbon Dust Of Planetary Nebula." 1–9.
- [11] Ji, C., Zhou, Y., Leblanc, R.M., and Peng, Z. (2020) "Recent Developments of Carbon Dots in Biosensing: A Review." ACS Sensors. 5 (9), 2724–2741.
- [12] Sanchís, J., Aminot, Y., Abad, E., Jha, A.N., Readman, J.W., and Farré, M. (2018) "Transformation of C60 Fullerene Aggregates Suspended and Weathered under Realistic Environmental Conditions." Carbon. 128 54–62.
- [13] Scott, L.T. (2004) "Methods for the Chemical Synthesis of Fullerenes." Angewandte Chemie - International Edition. 43 (38), 4994–5007.
- [14] Nimibofa, A., Newton, E.A., Cyprain, A.Y., and Donbebe, W. (2018) "Fullerenes: Synthesis and Applications." Journal of Materials Science Research. 7 (3), 22.
- [15] (2018) "C60 Fullerene Accumulation in Human Leukemic Cells and Perspectives of LED-Mediated Photodynamic Therapy." Free Radical Biology and Medicine. 124 319–327.
- [16] (2019) "Charged Clusters of C60 and Au or Cu Evidence for Stable Sizes and Specific Dissociation Channels.Pdf." J. Phys. Chem. A (123), 4599–4608.
- [17] Ganash, E.A., Al-Jabarti, G.A., and Altuwirqi, R.M. (2020) "The Synthesis of Carbon-Based Nanomaterials by Pulsed Laser Ablation in Water." Materials Research Express. 7 (1), 015002.
- [18] Alani, B.M.A. and Alalousi, M.A. (2021) "Structural, Morphological, and Spectroscopical Properties of Fullerenes (C60) Thin Film Prepared via Electrospray Deposition." Journal of Physics: Conference Series. 1829 (1),.
- [19] Khalil, L.S. and Alalousi, M.A. (2023) "Preparation and Characterization of Fullerene-AuNPs Composite Films.Pdf." Iraqi Journal of Applied Physics. 19 (4), 167–170.
- [20] Ali, H.H. and Alalousi, M.A. (2023) "Initial Characterization of the Prepared Au-Decorated TiO2:Fullerene Films Using Electrospray Method." Iraqi Journal of Applied Physics. 19 (4B), 151–156.
- [21] Ravelo-Nieto, E., Duarte-Ruiz, A., Reyes, L.H., and Cruz, J.C. (2021) "Synthesis and Characterization of a Fullerenol Derivative for Potential Biological Applications." (45), 15.
- [22] Serda, M., Gawecki, R., Dulski, M., Sajewicz, M., Talik, E., Szubka, M., et al. (2022) "Synthesis and Applications of [60]Fullerene Nanoconjugate with 5-Aminolevulinic Acid and Its Glycoconjugate as Drug Delivery Vehicles." RSC Advances. 12 (11), 6377–6388.
- [23] Mironov, G.I. (2019) "Electronic Structure and Optical Absorption Spectra of Gold Fullerenes Au16 and Au20." Physics of the Solid State. 61 (6), 1144–1153.
- [24] Du, C., Jin, K., and Liu, X. (2020) "Electronic and Optical Properties of Gold-Doped Endohedral Fullerenes." Journal of Materials Science. 55 (27), 12980–12994.
- [25] Zhao, W., Jones, R.M., D'Agosta, R., and Baletto, F. (2022) "Making Copper, Silver and Gold Fullerene Cages Breathe." Journal of Physics Condensed Matter. 34 (22),.
- [26] Unold, T. and Gütay, L. (2016) Photoluminescence Analysis of Thin-Film Solar Cells. in: D. Abou-Ras, T. Kirchartz, U. Rau (Eds.), Adv. Charact. Tech. Thin Film Sol. Cells, Second Edi, Wiley- VCH

- Verlag GmbH & Co. KGaA., pp. 275–297.
- [27] Reshchikov, M.A. (2021) "Measurement and Analysis of Photoluminescence in GaN." Journal of Applied Physics. 129 (12),.
- [28] Iwasiewicz-wabnig, A. (2007) Studies of carbon nanomaterials based on fullerenes and carbon nanotubes, Umeå University, 2007.
- [29] Bayramov, A.I., Mamedov, N.T., Dzhabfarov, T.D., Aliyeva, Y.N., Ahmadova, K.N., Alizade, E.H., et al. (2019) "Photoluminescence and Optical Transitions in C60 Fullerene Thin Films Deposited on Glass, Silicon and Porous Silicon." Thin Solid Films. 690 (May 2018), 137566.
- [30] Pattabi, M. and Pattabi, R.M. (2014) "Photoluminescence from Gold and Silver Nanoparticles." Nano Hybrids. 6 1–35.

دراسة خواص أغشية مترابك Fullerene/GNPs

لارا سعد خليل و مازن عبد الحميد الألوسي

جامعة الانبار/ كلية العلوم/ قسم الفيزياء/ الرمادي / العراق

الخلاصة:

خلاصة البحث بشكل واضح ودقيق ومعبر عن أفضل النتائج المستحصلة من هذه الدراسة وخلاصة الاستنتاجات وتكتب بلغة علمية بما يتوافق مع ما مكتوب باللغة الإنكليزية في هذا البحث على ان لا تتجاوز 150 كلمة.

تم تحضير أغشية مترابك جسيمات الفوليرين وجسيمات الذهب النانوية باستخدام تقنيتي الاستئصال بالليزر والرش الكهربائي. تم استخدام ليزر Nd-YAG النبضي بطول موجي 1064 نانومتر وطاقة 100 مللي جول لتحضير المحاليل الغروية، والتي تم رشها بجهاز رش كهربائي على قواعد ترسيب من الكوارتز عند درجة حرارة 300 ± 20 درجة مئوية. تم توصيف الأغشية المحضرة باستخدام حيود الأشعة السينية (XRD)، المجهر الإلكتروني الماسح (SEM)، مقياس الطيف الضوئي UV-VIS، والتألق الضوئي لدراسة خصائصها الهيكلية والمورفولوجية والبصرية، على التوالي. وأظهرت الأغشية المحضرة أطوار متعددة من C60 و C70، مع ملاحظة وجود اختلافات في التوزيع على أساس تركيز جزيئات الذهب النانوية. بالإضافة إلى ذلك، هناك عدة فجوات طاقة لكل غشاء اعتماداً على سلوك الامتصاص الذي ظهر ضمن مدى الطول الموجي (200–900) نانومتر، حيث تراوحت قيمها من (1.95 إلى 5.62) إلكترون فولت تبعاً للطور المتكون. في هذه الأثناء، أظهرت أطياف التألق الضوئي أربع قمم لكل غشاء، مع تأثير تركيز جسيمات الذهب النانوية على مواقع قمم الانبعاث وظهور القمم التي تتجاوز 500 نانومتر تزامناً مع اضافة الذهب الى المترابك.

الكلمات المفتاحية: Fullerene, Laser ablation, Electrospray, PL, UV-VIS